Electron generation in laser-irradiated insulators: theoretical desriptions and their application

Bärbel Rethfeld and Stefan Linden
Technische Universität Kaiserslautern, Germany

L. Englert, M. Wollenhaupt, L. Haag, C. Sarpe-Tudoran and T. Baumert
Universität Kassel, Germany

ABSTRACT

Transparent solids may absorb energy from a laser beam of sufficient high intensity. Several models are under consideration to describe the evolution of the free-electron density. Some of these models keep track of the energy distribution of the electrons. In this work we compare different models and give rules to estimate which one is applicable. We present the inclusion of a term in the multiple rate equation approach, recently introduced, describing fast recombination processes to exciton states. Moreover, we present experimental results with temporally asymmetric femtosecond laser pulses, impinging on a surface of fused silica. We found different thresholds for surface material modification with respect to an asymetric pulse and its time reversed counterpart. This difference is due to a different time-and-intensity dependence of the main ionization processes, which can be controlled with help of femtosecond shaped laser pulses.

Keywords: femtosecond laser absorption, dielectrics, avalanche, rate equation, pulse shaping, material processing, control

1. INTRODUCTION

Interaction of dielectrics with ultrashort laser pulses is a broad field of fundamental theoretical and experimental investigations stimulated also by the high potential of femtosecond laser pulses in applications like micro-machining and medical surgery.[1-3] When transparent solids are irradiated with laser intensities above a certain threshold, strong absorption of laser energy occurs, known as laser-induced breakdown. The increasing absorptivity is caused by the formation of a free electron gas in the conduction band of the dielectric. With the advent of ultrashort laser pulses of subpicosecond duration, a new regime of laser-matter interaction was opened where the pulse duration compares with characteristic times of microscopic collision processes within the material. Theoretical works study these microscopic processes and their influence on the free-electron distribution by solving kinetic equations like Fokker-Planck equation or Boltzmann equation.[4-7] Numerous experimental studies investigate processes like optical breakdown, filamentation and Coulomb explosion, see for example Refs. 8–14. For all kinds of practical investigations the pre-breakdown regime is of essential interest to monitor the evolution of the free-electron density and to control the laser induced damage. The temporal evolution of the free-electron density in a dielectric during ultrashort pulse laser irradiation plays therefore a fundamental role in these investigations. Usually for its description a simple rate equation is applied, though explicit kinetic calculations have shown its inadequacy on ultrashort time-scales.[6,15,16]

For a long time there was a gap between the oversimplified approach of the standard rate equation and the full kinetic treatment considering the microscopic collision processes in detail. In a recent Letter[17] I have introduced the multiple rate equation (MRE), which keeps track of the energy distribution of the free electrons, while maintaining the conceptual and analytic simplicity of the standard rate equation. It allows to calculate the temporal evolution of the free-electron density on a broad range of time-scales. The asymptotic solution of the multiple rate equation provides a possibility to calculate directly the avalanche parameter entering the standard rate equation and provides the condition of its applicability. Here we will present new insights into the role

---

E-mail correspondence to rethfeld@physik.uni-kl.de

of the main ionization mechanisms, their mutual influence, the distinction between two fundamentally different ionization regimes and the transition between these regimes.

In the next section we shortly resume the multiple rate equation in comparison with the commonly applied standard rate equation. Section 3 shows up in which regimes the distinct energy of electrons has to be considered. f.e. in frames of the multiple rate equation, and where the standard rate equation may be sufficient. In section 4 we show the influence of fast exciton recombination on the asymptotic behavior of free-electron density increase. Section 5 is devoted to an experimental result, revealing different damage thresholds for different pulse shapes at identical fluence, spectrum and statistical pulse duration. This difference is explained with the time-and-intensity dependence of the main ionization processes.

2. MULTIPLE RATE EQUATION

Classically, the free-electron generation in dielectrics is described by a simple rate equation for the increase of the total free electron density inherent in the conduction band, n_{total}:

$$\frac{dn_{\text{total}}}{dt} = \dot{n}_{\text{pi}}(E_L) + \alpha(E_L) \, n_{\text{total}} \; . \tag{1}$$

This equation combines the probability of photoionization $\dot{n}_{\text{pi}}$, directly depending on the amplitude of the electric laser field E_L, with the rate of impact ionization, assumed to depend on the total free electron density.

Due to photoionization electrons are shifted from the valence band into the conduction band.[18] In contrast, electron–electron impact ionization is caused by a free electron already existing in the conduction band. If its kinetic energy is sufficiently large, it may transfer part of it to an electron in the valence band, such that the latter is enabled to overcome the ionization potential.[19,20] The avalanche coefficient α depends on the effective energy gain of the free electron in the electric laser field E_L and can be intuitively estimated[21,8] by

$$\alpha_{\text{est}} = W_{\text{1pt}}(E_L) \, \hbar\omega_L / \varepsilon_{\text{crit}} \; . \tag{2}$$

Here, $W_{\text{1pt}}(E_L)$ is the probability of one-photon intraband-absorption, $\hbar\omega_L$ the photon energy of the laser light and $\varepsilon_{\text{crit}}$ is the critical energy for impact ionization. which is on the order of E_{gap}, the band gap between valance band and conduction band. A correction of this estimation, providing a possibility to *calculate* the avalanche parameter α was found in Ref. 17 and will be given below.

Equation (1) was proposed and verified for laser pulses in the nanosecond regime (see for instance Refs. 22,23 and references therein). Experiments measuring the optical breakdown threshold (OBT) for different pulse durations down to the femtosecond regime were analyzed by using eq. (1). identifying the electronic avalanche as the *dominant* excitation mechanism, while multiphoton absorption only provides seed electrons for this avalanche.[4,11] However, in Ref. 13 single-shot time-resolved experiments were performed to study the free-electron density evolution in dielectrics, probing also the electron density below OBT. These experiments could only be successfully interpreted when *neglecting* the contribution of the electron avalanche, i.e. the second term in eq. (1).

Thus, experimental studies applying eq. (1) have lead to contradictory results. Moreover, theoretical investigations state fundamental doubts whether this standard rate equation is applicable in general in the subpicosecond time regime.[6,15,16] One basic assumption of eq. (1) is that impact ionization depends directly on the total density of the free electrons. However, impact ionization needs a certain critical energy of the ionizing electron. thus this process depends also on the *energy* of a particular electron in the conduction band. While photoionization generates electrons with *low* kinetic energy in the conduction band. impact ionization requires electrons of *high* kinetic energy. This additional energy is absorbed from the laser light by intraband absorption. If this absorption process takes time comparable to the laser pulse duration, it is obvious that eq. (1) is oversimplified. On ultrashort time scales the shape of the electron distribution in the conduction band may change in time; then the energy-averaged total electron density, n_{total} is not an adequate parameter to describe the ionization process. At least until the shape of the transient distribution function of the electrons in the conduction band becomes stationary. the energy distribution of the electrons is crucial for the probability of impact ionization.

Defining the density n_k of electrons above $\varepsilon_{\text{crit}}$, where k will be identified with the number of photons necessary to reach $\varepsilon_{\text{crit}}$, a modified rate equation can be formulated as

$$\frac{dn_{\text{total}}}{dt} = \dot{n}_{\text{pi}}(E_L) + \tilde{\alpha}\,n_k\ ,\tag{3}$$

where $\tilde{\alpha}$ represents the direct probability for impact ionization, provided that an electron with sufficient energy exists in the conduction band. $\tilde{\alpha}$ can be estimated from the corresponding collision term given for example in Ref. 6 and is, in contrast to the avalanche parameter $\alpha(E_L)$ independent of laser parameters. In case of a stationary shape of the electron distribution in the conduction band, the fraction of high-energy electrons n_k/n_{total} is temporally constant and the modified rate equation (3) reduces to the standard rate equation (1) with $\alpha(E_L) = \tilde{\alpha}\,n_k/n_{\text{total}}$. For the non-stationary case, the fraction of high-energy electrons changes with time and the difference in the last term of Eq. (3) as compared to Eq. (1) is substantial.

Equation (3) follows directly from the multiple rate equation (MRE), introduced in Ref. 17. It provides a possibility to calculate the density of high-energy electrons $n_k(t)$ and thus the transient evolution of free electron density $n_{\text{total}}(t)$ also for the highly non-stationary regime on ultrashort time-scales. The MRE is a comparably simple description which keeps track of the electrons energy distribution, as up to now only realized by complex kinetic approaches, while maintaining the conceptual simplicity of the standard rate equation. It is given by

$$
\begin{aligned}
\dot{n}_0 &= \dot{n}_{\text{pi}} + 2\,\tilde{\alpha}\,n_k - W_{1pt}\,n_0 \\
\dot{n}_1 &= W_{1pt}\,n_0 - W_{1pt}\,n_1 \\
\dot{n}_2 &= W_{1pt}\,n_1 - W_{1pt}\,n_2 \\
&\vdots \\
\dot{n}_{k-1} &= W_{1pt}\,n_{k-2} - W_{1pt}\,n_{k-1} \\
\dot{n}_k &= W_{1pt}\,n_{k-1} - \tilde{\alpha}\,n_k\ ,
\end{aligned}
\tag{4}
$$

$$\text{with}\qquad k = \left\lfloor \frac{\varepsilon_{\text{crit}}}{\hbar\omega_L} + 1\right\rfloor\ .$$

Here, n_j denotes the density of electrons at a discrete energy level ε_j. The $k+1$ energy levels ε_j are given by $\varepsilon_0 \approx 0$, $\varepsilon_{j+1} = \varepsilon_j + \hbar\omega_L$, where $k = \lfloor \varepsilon_{\text{crit}}/\hbar\omega_L + 1\rfloor$ is the integer part of $\varepsilon_{\text{crit}}/\hbar\omega_L + 1$ and denotes the minimum number of photons necessary to be absorbed by an electron at $\varepsilon_0 \approx 0$ to reach the critical energy for impact ionization $\varepsilon_{\text{crit}}$.

The formulation (4) of the MRE is based on a simplified view of the energy dependence of the main processes involved in the generation of free electrons in the conduction band (CB) of a dielectric, which is sketched in Fig. 1. Photoionization is assumed to generate electrons at the lower edge of the conduction band. With a certain probability W_{1pt}, which generally may depend on energy ε_j, such electron may absorb further single photons from the laser light and gradually reach the critical energy necessary for impact ionization. After that the electron's kinetic energy is reduced and a second electron is shifted from the valence band (VB) into the conduction band. Both electrons then have a small kinetic energy, which can be assumed to be comparable to ε_0, starting the cycle of ionization anew.

Here, relaxation processes as electron–electron relaxation and electron–phonon interaction have been neglected in order to extract the *main* effect of energy dependence of the ionization processes, leading to the failure of eq. (1) on ultrashort time-scales. While electron–electron relaxation simply smears out the peaks in the electron distribution (see for example Fig. 3 in Ref. 6), electron–phonon interaction leads on picosecond and larger time-scales to energy loss of the electron system. The reduced energy increase of the electrons during irradiation may be included qualitatively by modifying the probability $W_{1pt}(\varepsilon_j)$ to an *effective* probability of energy increase.

In general cases the probability of impact ionization $\tilde{\alpha}$ is much larger than the one-photon absorption probability W_{1pt}. For the transition $\tilde{\alpha} \to \infty$ the last equation of (4) becomes redundant and instead of the term $+2\tilde{\alpha}\,n_k$
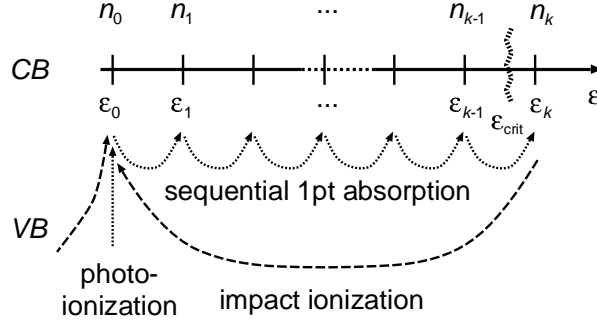
Figure 1. Schematic view of the processes providing changes in the density and the energy, respectively, of free electrons in the conduction band of a dielectric.

in the first equation a term $+2\,W_{1\text{pt}}\,n_{k-1}$ may be used. This modification of the MRE (4) was applied in Ref. 24. it leads to a simplified numerical handling of the MRE.

As presented in Ref. 17, the MRE can be solved analytically with help of Laplace transform. For the case of $\tilde{\alpha} \gg W_{1\text{pt}}$, which is a similar but weaker assumption than the often applied "flux-doubling" model,[4,7] the solution can be found analytically. It consists of a sum of exponential functions; the largest of them takes over for long times and provides the asymptotic solution which reads

$$n_{\text{total}}(t) = \frac{\dot{n}_{\text{pi}}/W_{1\text{pt}}}{2k(\sqrt[k]{2} - 2 + \sqrt[k]{1/2})} \times \exp\left[t\,/\,t_{\text{MRE}}\right] \tag{5}$$

and is valid for $t \gg t_{\text{MRE}}$ with

$$t_{\text{MRE}} = [(|\sqrt[k]{2}| - 1)\,W_{1\text{pt}}]^{-1} \ . \tag{6}$$

Here, constant intensity and thus constant ionization probabilities have been assumed.

The "transition time" t_{MRE} characterizes the transition between the non-stationary regime on ultrashort time-scales and the asymptotic avalanche regime for longer times, described by Eq. (5) with the avalanche parameter

$$\alpha_{\text{asymp}} = 1/t_{\text{MRE}} = (|\sqrt[k]{2}| - 1)\,W_{1\text{pt}} \ . \tag{7}$$

The above mentioned estimated avalanche parameter α_{est}, eq. (2), compares with the limit for $k \to \infty$ of $\alpha_{\text{asymp}} \to \ln(2)\,W_{1\text{pt}}/k$. Thus, α_{est} is about a factor $\ln(2)^{-1}$ larger than the *calculated* value α_{asymp}. This factor accounts in the latter value for the *doubling* of electrons in each impact ionization event.

In case of $W_{1\text{pt}}$ depending on kinetic energy ε_j, the asymptotic behavior is similar to solution (5) with an exponent. i.e. an avalanche coefficient α. given by the largest positive real root of the polynomial

$$p(s) = (s + \tilde{\alpha}) \cdot \prod_{j=1}^{k-1} (s + W_{1\text{pt}}(\varepsilon_j)) - 2\tilde{\alpha} \cdot \prod_{j=1}^{k-1} W_{1\text{pt}}(\varepsilon_j) \ . \tag{8}$$

3. TIME-AND-INTENSITY DEPENDENCE OF IONIZATION PROCESSES

For the following examples of results obtained in 25. a laser with photon energy $\hbar\omega_L = 2.48$ eV and electric field amplitudes up to $E_L = 1 \times 10^{10}$ V/m was assumed, leading for a material with $E_{\text{gap}} = 9$ eV to a critical energy of impact ionization between 13.5 and 14.5 eV.[17] hence, $k = 6$. The probability of impact ionization $\tilde{\alpha}$ was estimated from the corresponding collision term in Ref. 6 as $\tilde{\alpha} = 1 \times 10^{15}$ s^{-1}. The rate of photoionization $\dot{n}_{\text{pi}}$

is taken from Ref. 18, $W_{1\text{pt}}$ is chosen to be $3.5 \times 10^{-7}\ E_L^2\ \text{m}^2/\text{V}^2\text{s}$, which compares well with the mean value of the one-photon absorption probability for SiO_2 in Refs. 26,6. These material parameters correspond roughly to the case of SiO_2, however. the results presented in the following are of general character. Peculiarities of quartz as ultrafast recombination in self-trapped exciton states[27,28] were neglected. A possibility of their inclusion is presented in section 4.

3.1. Non-stationary regime

At the initial stage of ionization, the fraction of electrons with energies sufficient to perform impact ionization is expected to be small due to the non-vanishing time necessary for intraband absorption. Thus, at this stage. photoionization is the dominating ionization process. Later, the shape of the free electron distribution becomes stationary and the probability of impact ionization. which depends on the density of high-energy electrons n_k, may be expressed through the total electron density n_{total}.
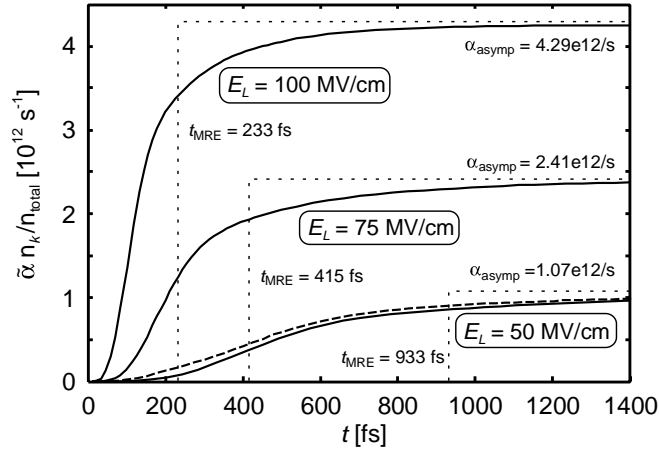

Figure 2. Temporal evolution of the fraction of high-energy electrons $\tilde{\alpha} n_k / n_{\text{ges}}$ for different laser field amplitudes calculated by the MRE (4) (solid lines). The asymptotical values coincide with the avalanche coefficient α_{asymp}, eq. (7). For times up to the range of t_{MRE} the fraction of high-energy electrons strongly changes in time. The dashed line shows the normalized fraction of high-energy electrons calculated with the full kinetic approach from Ref.[6] for $E_L = 50\ \text{MV/cm}$.

The transient fraction of high-energy electrons n_k / n_{total} (multiplied with $\tilde{\alpha}$) is shown in Fig. 2. It reflects the temporal evolution of the shape of the free-electron distribution function for ultrashort times and its development towards the asymptotic stationary long-time behavior. Depending on electric laser field, the time to reach the stationary regime and thus a constant fraction of high-energy electrons is in the range of several hundreds of femtoseconds. Below this timescale the fraction of high energy electrons is much lower than its asymptotic value. Fig. 2 shows also the normalized fraction of electrons with energy above $\varepsilon_{\text{crit}}$ resulting from the full kinetic calculation of Kaiser et al.[6] for an electric field of $E_L = 50\ \text{MV/cm}$. The transient non-stationary electron distribution is very well imitated by the MRE model (4). For times much larger than t_{MRE}, when the stationary regime is reached and equation (1) can be assumed to be valid, the fraction $\tilde{\alpha} n_k / n_{\text{total}}$ provides the avalanche coefficient for eq. (1), compare eq. (3). The dotted lines in Fig. 2 correspond to the analytically calculated asymptotic value of $\alpha(E_L)$ according to eq. (7), assumed to be valid after $t \gg t_{\text{MRE}}$. The MRE model (4) thus provides a comparably simple possibility both to consider the non-stationary electron distribution in dielectrics during ultrashort laser irradiation and to follow the transition to the asymptotic avalanche regime for longer times.

3.2. Contribution of impact ionization

A question of great interest is the fraction of impact ionized electrons electrons provided through impact ionization $n_{\mathrm{imp}}/n_{\mathrm{total}}$ as a function of duration and intensity.

The multiple rate equation was solved in Ref. 17 for the case $\tilde{\alpha} \gg W_{\mathrm{1pt}}$ with help of the Laplace transform. Performing the transition $\tilde{\alpha} \to \infty$ and thus neglecting the last equation in equation system (4), the $\mathcal{L}$-transformed function η_{k-1} of n_{k-1} reads

$$\eta_{k-1}(s) = \frac{W_{\mathrm{1pt}}^{k-1}}{(s + W_{\mathrm{1pt}})^k - 2W_{\mathrm{1pt}}^k} \cdot \frac{\dot{n}_{\mathrm{pi}}}{s} \; , \tag{9}$$

with the $k+1$ poles $s_0 = 0$, and $s_{1..k} = (\sqrt[k]{2} - 1) W_{\mathrm{1pt}}$. The full solution reads

$$n_{k-1}(t) = -\frac{\dot{n}_{\mathrm{pi}}}{W_{\mathrm{1pt}}} + \sum_{i=1..k} \frac{\dot{n}_{\mathrm{pi}}}{W_{\mathrm{1pt}}} \frac{1}{K_i^*} \exp[s_i\, t] \; , \tag{10}$$

with $K_i^* = 2k(1 - \sqrt[k]{1/2})$, leading to the solution for the total free electron density:

$$n_{\mathrm{total}}(t) = \frac{\dot{n}_{\mathrm{pi}}}{W_{\mathrm{1pt}}} \sum_{i=1..k} \frac{1}{K_i} \times \exp[s_i\, t] \; , \tag{11}$$

with $K_i = 2k \left(\sqrt[k]{2} - 2 + \sqrt[k]{1/2} \right)$.

Obviously, for constant intensity the density of electrons provided by photoionization is given by

$$n_{\mathrm{pi}}(t) = \dot{n}_{\mathrm{pi}}t \; . \tag{12}$$

For the fraction of impact electrons follows the dependence:

$$\frac{n_{\mathrm{imp}}}{n_{\mathrm{total}}} = \frac{n_{\mathrm{total}}(t) - \dot{n}_{\mathrm{pi}}t}{n_{\mathrm{total}}(t)} = \frac{\sum 1/K_i \cdot \exp[s_i\, t] - W_{\mathrm{1pt}} \cdot t}{\sum 1/K_i \cdot \exp[s_i\, t]} \; . \tag{13}$$

As long as W_{1pt} is proportional to the intensity I_L, which is given f.e. for the case of Drude-like absorption, the equation (13) depends only on the product $I_L \cdot t$, given in 10 Ws/cm^2 for the dashed line. The self-similarity can be used for instance to calculate the transition time t_{MRE}, which divides the region of domination of photoionization from the avalanche dominated regime. For the given laser and material parameters the transition time may be expressed as $t_{\mathrm{MRE}} \simeq 10^{13}/I_L$ ps W/cm^2.

Figure 3 shows percentiles of the fraction of impact ionized electrons electrons provided through impact ionization $n_{\mathrm{imp}}/n_{\mathrm{total}}$ as a function of duration and intensity. The transition time t_{MRE} marks the transition between the non-stationary short-time regime for short pulses and low intensities where photoionization is dominating and the asymptotic long-time regime for long pulses and high intensities where the impact avalanche is governing the free electron generation, respectively.

3.3. Choice of description

Figure 3 provides a possibility to distingiush between different theoretical desriptions, applicable in different time-and-intensity regimes. For short pulses and low intensities, were multiphoton ionization dominates, an inclusion of *only* the photoionization term in (1) (or (4), what is the same in this case) is sufficient. For the asymptotic regime of collisional avalanche, i.e. for long pulses and higher intensities, the usage of the standard rate equation (1) is justified. In the intermediate regime around t_{MRE} given by Eq. (6), the full equation system of MRE (4) must be applied. The multiple rate equation covers also both other regimes and can be considered as a general description.
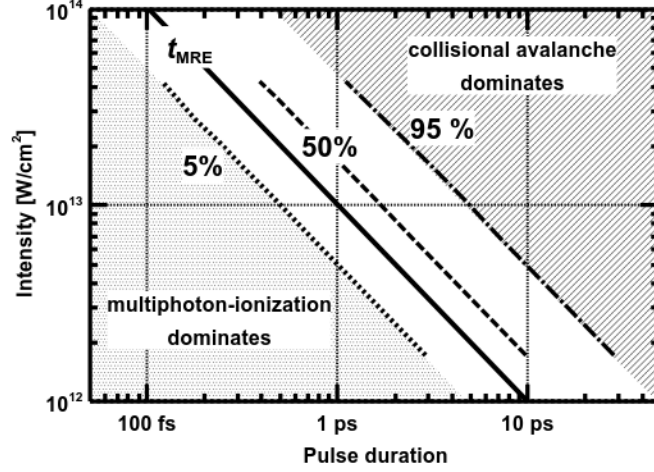
Figure 3. Percentiles of the fraction of impact ionized electrons $n_{\mathrm{imp}}/n_{\mathrm{total}}$ in dependence on laser intensity and pulse duration. $I_L - t$ regions where either of the ionization processes is dominating are shaded. The transition time t_{MRE} marks the transition between photoionization–dominated regime and avalanche dominated regime.

4. INCLUSION OF RECOMBINATION

In[17,25] the evolution of the free-electron density was studied for the case of irradiation of SiO_2 on timescales in the femto- to picosecond range. However, recombination processes were neglected, though they may play a considerable role. Especially for quartz, fast recombination processes on a timescale of about 150 fs are known; here ultrafast recombination in self-trapped exciton states have been experimentelly found.[28,27]

Generally, recombination may be included in the multiple rate equation analogously to the extension of the standard rate equation as proposed in Refs..[14,29] Aiming to calculate the stationary long-time behavior, we allow for re-excitation from the exciton states with a probability W_{exc}. With the recombination time τ_{recomb} a modified MRE may be formulated as:

$$
\begin{aligned}
\dot{n}_{\mathrm{exc}} &= n_{\mathrm{total}}/\tau_{\mathrm{recomb}} - W_{\mathrm{exc}} n_{\mathrm{exc}} \\
\dot{n}_0 &= \dot{n}_{\mathrm{pi}} + 2\,\tilde{\alpha}\,n_k - W_{1pt}\,n_0 \\
&\quad + W_{\mathrm{exc}} n_{\mathrm{exc}} - n_0/\tau_{\mathrm{recomb}} \\
\dot{n}_1 &= W_{1pt}\,n_0 - W_{1pt}\,n_1 - n_1/\tau_{\mathrm{recomb}} \\
\dot{n}_2 &= W_{1pt}\,n_1 - W_{1pt}\,n_2 - n_2/\tau_{\mathrm{recomb}} \\
&\quad\vdots \\
\dot{n}_{k-1} &= W_{1pt}\,n_{k-2} - W_{1pt}\,n_{k-1} - n_{k-1}/\tau_{\mathrm{recomb}} \\
\dot{n}_k &= W_{1pt}\,n_{k-1} - \tilde{\alpha}\,n_k - n_k/\tau_{\mathrm{recomb}}\ ,
\end{aligned}
\tag{14}
$$

where n_{exc} is the density of electrons in exciton states, $n_{\mathrm{total}} = \sum_i n_i$ and n_k the density of high-energy electrons, as in section 2 where also the other quantities are given.

Fig. 4 shows the transient fraction of high-energy electrons, which reflects the evolution of the shape of the free-electron distribution from the initial nonstationary behavior towards the asymptotic stationary long-time behavior. A constant laser field amplitude of $E_L = 100$ MV/cm was chosen and the normalized fraction $\tilde{\alpha} n_k/n_{\mathrm{total}}$
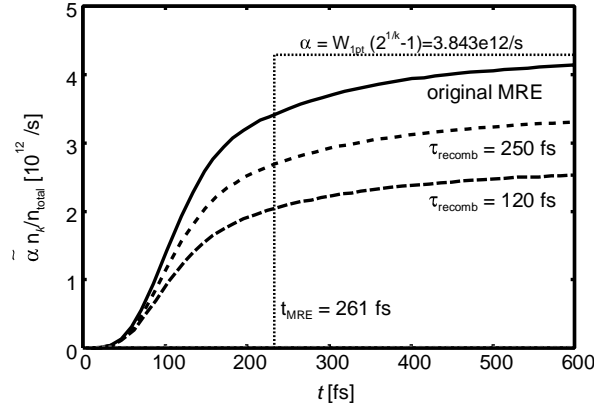
Figure 4. Development to asymptotic behavior including different recombination times. The solid curve corresponds to the original MRE, while the dashed lines give the avalanche parameter including different recombination times as indicated.

was calculated with the original MRE (solid line) and including recombination with different characteristic recombination times (dashed lines), respectively. For the calculation we assumed $W_{\mathrm{exc}} = W_{\mathrm{1pt}}$. While the resulting asymptote strongly depends on the recombination time. the time to reach the stationary regime, t_{MRE}, does not. The dotted line shows the corresponding results of the analytical estimation based on the Laplace transform of the unmodified MRE, i.e. the asymptotic value of the avalanche parameter and the transition time t_{MRE}. Seminumerical estimations of the asymptotic avalanche parameter including recombination depend on material and laser parameters.[30]

Thus, while the asymptote itself, i.e. the avalanche parameter which under certain conditions can be inserted in Eq. (1), is depending strongly on the recombination time, the characteristic time to *reach* the asymptotic regime is nearly uneffected and can be assumed to be given by Eq. (6), also if fast recombination processes influence the free electron density.

5. EXPERIMENTAL AND THEORETICAL STUDIES OF THE EFFECT OF PULSESHAPE

In the following we present experimental studies with temporally asymmetric pulse shapes, enabling us to control the temporal evolution of the free-electron density. We reveal a systematic dependence of the damage threshold on the laser pulse shape for different dielectric materials. Accompanying calculations, using the multiple rate equation (4) show that the characteristics of the free-electron density increase as well as its final value strongly depends on the laser pulse shape.

We obtain our experimental results by introducing third order dispersion (TOD) via spectral phase modulation in a pulse shaper buildt at the University of Kassel, Germany.[31] Analytic formulas for cubic phase shaped laser pulses of the form $\Phi(\omega) = \frac{\Phi_3}{3!}(\omega - \omega_0)^3$ where Φ_3 is termed TOD and ω_0 is the central frequency and can be found in 32,33. The experimental setup was described elsewhere.[34,35] Here we present the results of material modification on a surface of fused silica.

Fig. 5 shows SEM micrographs of damage structures on fused silica. A triplet of applied laser pulses with different third order dispersion (TOD)s (negative Φ_3. zero Φ_3 and positive Φ_3) for a fixed energy and focal position is highlighted. For all Φ_3 the pulses have the same energy, spectral intensity and spatial profile. The positive
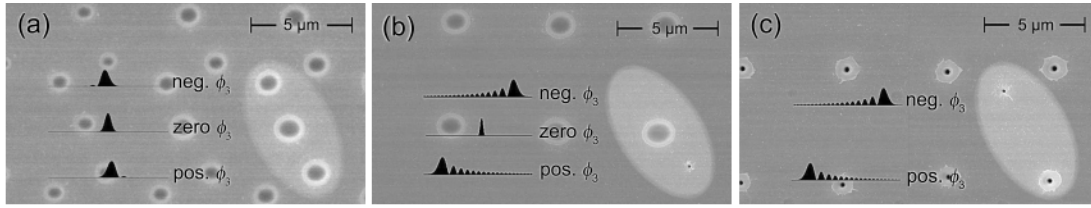
Figure 5. Scanning electron microscope micrographs of a measurement pattern on fused silica: For an applied energy and focal position a triplet of applied laser pulses is highlighted by the ellipse. Negative, zero and positive TOD were used. Normalized temporal intensity profiles are sketched for comparison between different TODs. (a) low TOD ($\phi_3 = \pm 2.5 \cdot 10^4$ fs^3, $E = 77$ nJ) results in negligible differences between created structures. (b) high positive TOD ($\phi_3 = +6 \cdot 10^5$ fs^3, $E = 71$ nJ) results in a change of structure size and threshold energy. The threshold energy for ablation with negative TOD ($\phi_3 = +6 \cdot 10^5$ fs^3) is reached in (c) with $E = 110$ nJ. Here the unshaped pulse is suppressed in order not to mask structures with TOD.

and negative phase mask have the same pulse duration but their time profile is time-inverted. Fig. 5a shows structures resulting from a weak TOD of $\Phi_3 = \pm 2.5 \cdot 10^4$ fs^3 leading to no significant changes neither to the diameter nor to threshold (not shown) for material processing. The statistic pulse duration of $2\sigma = 50$ fs is only slightly longer compared to the bandwidth limited pulse of 35 fs. For a strong TOD of $\phi_3 = +6 \cdot 10^5$ fs^3 (see Fig. 5b) the statistic pulse length raises to $2\sigma = 960$ fs. The highlighted triplet is at the threshold energy (71 nJ) for material processing with positive Φ_3. For $\phi_3 = -6 \cdot 10^5$ fs^3 the first structures appear at 110 nJ (Fig. 5c) and look similar to the structures for positive Φ_3. In this pulse energy region unshaped pulses are suppressed in order not to mask structures with TOD. The energies are measured single shot for the specified holes. Note within that context, that the energy transmission through the phasemodulator for positive and negative TOD measured at the entrange pupil of the objective is constant.

Here we concentrate our discussion on the difference in threshold energies for different signs of the cubic phase i.e. different asymmetric temporal pulse shapes. To that end we calculate the transient free-electron density in laser-irradiated dielectrics by making use of the multiple rate equation (MRE).[17] The achievement of a certain critical density is commonly accepted as a criterion for laser induced damage in dielectrics. In the following a remarkable difference in the transient evolution of electron density as well as in its final values is revealed for both signs of phase modulation.

We apply material parameters of fused silica and laser parameters as used in the experiments. The probability for intrabandabsorption for a laser wavelength of $\lambda = 790$ nm is assumed as $W_{1pt} = 1.38 \times 10^{-6}\ E_L^2$ m^2/V^{2}s, using the value in Ref.[17] and the Drude formula. Other material parameters are given in the preceding sections. Recombination[28,29] is neglected for the present study.

Fig. 6 shows the increase of total free electron density for negative and positive cubic phase. The corresponding asymmetric temporal intensity profiles are shown as dashed-dotted curves. Here, a pulse duration of $\Delta t = 35$ fs of the unperturbed pulse (FWHM) and a phase modulation with $|\phi_3| = 600\,000$ fs^3 were applied, resulting in a statistical pulse duration of $\sigma = 480$ fs. The resulting transient intensity is plotted for the case of $\phi_3 > 0$ and $\phi_3 < 0$ where for the latter case an offset of 4σ in time was used for better visualization.

In both cases, the density of electrons shifted to the conduction band by the process of photoionization n_{pi} is plotted additionally to the total free-electron density n_{total}. Fig. 6 shows a remarkable difference in the characteristic of free-electron density increase as well as in the finally reached value between both signs of the cubic phase. For the case of positive cubic phase the total free-electron density increases strongly at the beginning of irradiation. Later on, a further gradual increase is observed, attenuating at the end of the laser pulse. In contrast, for the case of negative cubic phase, the total free-electron density increases only by the end of irradiation, when
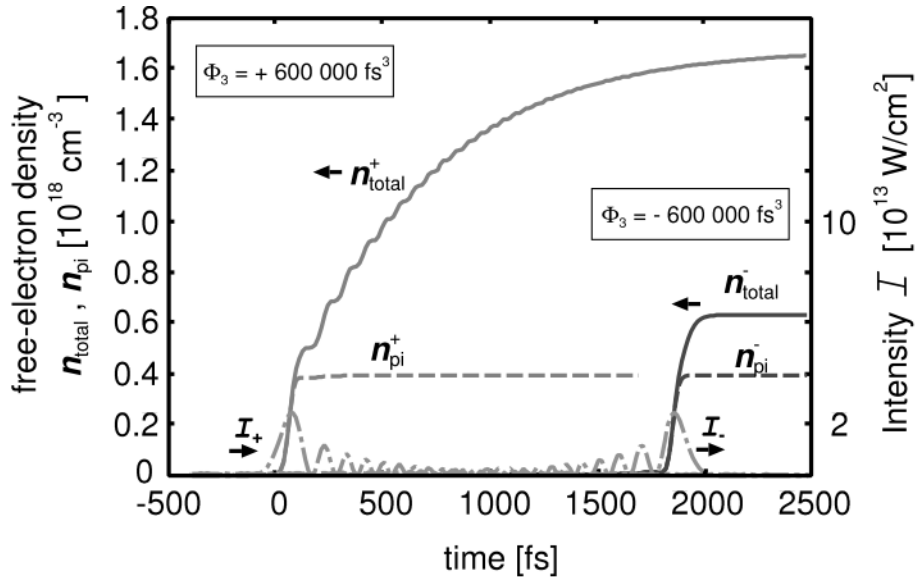
Figure 6. Transient free-electron density n_{total} (solid lines) as calculated with help of the MRE, together with the density of electrons provided by photoionization n_{pi} (dashed lines) and the corresponding transient intensities (dashed-dotted lines) of the positive modulated pulse (index +) and the negative modulated pulse (index -), respectively.

the peak intensity of the pulse train is reached. The finally reached value is lower than for the case of positive cubic phase.

The individual behavior for both pulse shapes is caused by a time effect together with the strong intensity-dependence of both ionization processes. Photoionization depends directly on intensity as I^ℓ in case of ℓ-photon ionization, therefore nearly all electrons are shifted to the conduction band during the peak intensity, which is reached at the beginning or at the end of irradiation, for the positive and negative cubic phase, respectively.

In the case of positive cubic phase, irradiation continues for a comparatively long time after the peak intensity, thus, the initially provided free-electrons are further heated and impact–ionization becomes possible. The Drude-like heating of free electrons depends on intensity as well (in this case the dependence is linearly, see above W_{1pt}), reflected by bumps in the density increase at the time of decreasing local intensity maxima of the positive cubic phase shaped laser pulse. In case of negative cubic phase, the gradually increasing intensity in the initial phase of the modulated pulse does not provide a remarkable density of electrons through multiphoton ionization, thus also impact ionization is inhibited. Only during the main peak at the *end* of the pulse train, photoionization becomes important, providing finally the same amount of free electrons as in the case of a positive phase mask. After the maximum intensity is reached, it steadily decreases within the main peak on a short timescale compared to the total pulse duration. During this intensity decrease only a small amount of free-electrons are provided by impact–ionization leading to a lower final free-electron density as compared to the positive-modulated laser pulse.

6. SUMMARY

In summary, a model has been developed to describe the free electron density evolution in the conduction band of a dielectric under ultrashort laser irradiation. In contrast to the commonly applied simple rate equation describing only the total density of free electrons, the model presented in this article and in Refs. 17,25 takes into account

also the *energy* of electrons in the conduction band. This is important for the ionization probability as long as the shape of electron distribution has not become stationary, i.e. in the femtosecond time regime up to picosecond timescales, depending on intensity, as the examples in this work have shown. The model leads to an ordinary differential equation system and ows much higher applicability than existing kinetic approaches. It thus provides a practical tool for such theoretical and experimental investigations where details of the collision processes are not required to know but the transient free electron density enters as a parameter.

We have studied the non-stationary regime where the fraction of free electrons with energy above critical energy for impact ionization is changing in time. The transition from the non-stationary regime to the asymptotic avalanche regime is governed by the transition time t_{MRE}, which is a function of laser intensity. The transition time may be used to decide which model is applicable. We have introduced fast recombination in our model and found that this process does not influence the transition time, however, the avalanche parameter changes, when the asymptotic avalanche regime is reached. The fraction of impact ionized electrons has been studied in dependence on laser intensity and pulse duration. Here, a self-similarity was revealed: the fraction of impact ionization depends on the *product* of intensity and duration of the laser pulse. Finally, experimental results with temporally asymmetric femtosecond laser pulses have shown a strong effect of laser pulse shape on the final material modification. Accompanying calculations show the influence of laser pulse shape on the transient characteristics of the free-electron density as well as on its final value, suggesting a remarkable influence of the laser pulseshape on dielectric breakdown. These differences are due to a different time-and-intensity dependence of the main ionization mechanisms. We thus propose to control these ionization processes by applying femtosecond shaped laser pulses.

REFERENCES

1. A. Vogel. J. Noack, G. Hüttman, and G. Paltauf. Mechanisms of femtosecond laser nanosurgery of cells and tissues. *Appl. Phys. B*, 81:1015, 2005.
2. C. L. Arnold, A. Heisterkamp, W. Ertmer, and H. Lubatschowski. Streak formation as side effect of optical breakdown during processing the bulk of transparent Kerr media with ultra-short laser pulses. *Appl. Phys. B*, 80:247–253, 2005.
3. F. Korte, J. Koch, and B.N. Chichkov. *Appl. Phys. A*, 79:879, 2004.
4. B. C. Stuart, M. D. Feit. S. Herman, A. M. Rubenchik. B. W. Shore, and M. D. Perry. Nanosecond-to-femtosecond laser-induced breakdown in dielectrics. *Phys. Rev. B*, 53(4):1749–1761, January 1996.
5. T. Apostolova and Y. Hahn. Modeling of laser-induced breakdown in dielectrics with subpicosecond pulses. *J. Appl. Phys.*, 88:1024, 2000.
6. A. Kaiser, B. Rethfeld, M. Vicanek, and G. Simon. Microscopical processes in dielectrics absorbing a subpicosecond laser pulse. *Phys. Rev. B*, 61(17):11437–11450, 2000.
7. S.R. Vatsya and S.K. Nikumb. Modeling of laser-induced avalanche in dielectrics. *J. Appl. Phys.*, 91:344, 2002.
8. L. Sudrie, A. Couairon, M. Franco. B. Lamouroux, B. Prade, S. Tzortzakis, and A. Mysyrowicz. Femtosecond laser-induced damage and filamentary propagation in fused silica. *Phys. Rev. Lett.*, 89:186601, 2002.
9. R. Stoian. M. Boyle, A. Thoss, A. Rosenfeld, G. Korn, I.V. Hertel, and E.E.B. Campbell. Laser ablation of dielectrics with temporally shaped femtosecond pulses. *Appl. Phys. Lett.*, 80:353, 2002.
10. A. C. Tien, S. Backus, H. Kapteyn, M. Murnane, and G. Mourou. Short-pulse laser damage in transparent materials as a function of pulse duration. *Phys. Rev. Lett.*, 82(19):3883, 1999.
11. M. Lenzner, J. Krüger, S. Sartania, Z. Cheng, G. Mourou Ch. Spielmann, W. Kautek, and F. Krausz. Femtosecond Optical Breakdown in Dielectrics. *Phys. Rev. Lett.*, 80(18):4076, 1998.
12. D. von der Linde and H. Schüler. Breakdown threshold and plasma formation in femtosecond laser-solid interaction. *J. Opt. Soc. Am.*, B13(1):216–222, January 1996.
13. F. Quere, S. Guizard, and Ph. Martin. Time-resolved study of laser-induced breakdown in dielectrics. *Europhys. Lett.*, 56:138, 2001.

14. M. Li, S. Menon, J.P. Nibarger, and G.N. Gibson. Ultrafast Electron Dynamics in Femtosecond Optical Breakdown of Dielectrics. *Phys. Rev. Lett.*. 82:2394–2397, 1999.

15. A. A. Manenkov and A. M. Prokhorov. Laser-induced damage in solids. *Sov. Phys. Usp.*, 29(1):104–122, January 1986.

16. N. Bityurin and A. Kuznetsov. Use of harmonics for femtosecond micromachining in pure dielectrics. *J. Appl. Phys.*, 93:1567, 2003.

17. B. Rethfeld. Unified Model for the Free-Electron Avalanche in Laser-Irradiated Dielectrics. *Phys. Rev. Lett.*, 92:187401, 2004.

18. L. V. Keldysh. Ionization in the field of a strong electromagnetic wave. *Sov. Phys. JETP*, 20:1307–1314, 1965.

19. L. V. Keldysh. Kinetic theory of impact ionization in semiconductors. *Sov. Phys. JETP*, 10:509–518, 1960.

20. N. Bloembergen. Laser-Induced Electric Breakdown in Solids. *IEEE J. Quantum Electron.*, QE-10(3):375, 1974.

21. A. Gaeta. Catastrophic Collapse of Ultrashort Pulses. *Phys. Rev. Lett.*, 84:3582–3585, 2000.

22. W.L. Smith. *Optical Eng.*, 17:489–503. 1978.

23. S.C. Jones, P. Bräunlich, R.T. Casper, X.-A. Shen, and P. Kelly. Recent progress on laser-induced modifications and intrinsic bulk damage of wide-gap optical materials. *Optical Eng.*, 28:1039–1068, 1989.

24. C. L. Arnold, A. Heisterkamp, W. Ertmer, and H. Lubatschowski. Numerical calculation of nonlinear ultrashort laser pulse propagation in transparent kerr media. *Proc. SPIE - Int. Soc. Opt. Eng. (USA)*, 5714:126–137, 2005.

25. B. Rethfeld. Free-electron generation in laser-irradiated dielectrics. *Phys. Rev. B*, 73:035101, 2006.

26. D. Arnold and E. Cartier. Theory of laser-induced free-electron heating and impact ionization in wide-band-gap solids. *Phys. Rev. B*, 46(23):15102–15115, December 1992.

27. G. Petite, P. Daguzan, S. Guizard, and P. Martin. Conduction electrons in wide-bandgap oxides: a sub-picosecond time-resolved optical study. *Nuclear Instruments and Methods in Physics Research, Section B*, 107:97–101, 1996.

28. P. Audebert, Ph. Daguzan, A. Dos Santos. J. C. Gauthier, J. P. Geindre, S. Guizard, G. Hamoniaux, K. Krastev, P. Martin. G. Petite, and A. Antonetti. Space-Time Observation of an Electron Gas in SiO_2. *Phys. Rev. Lett.*, 73(14):1990–1993, October 1994.

29. G. Petite, S. Guizard, P. Martin, and F. Quere. Comment on Ultrafast Electron Dynamics in Femtosecond Optical Breakdown of Dielectrics. *Phys. Rev. Lett.*. 83:5182, 1999.

30. Stefan Linden. Beschreibung der transienten Elektronendichte bei der Bestrahlung dielektrischer Festkörper mit ultrakurzen Laserpulsen. Technical University of Kaiserslautern, Germany, 2008.

31. A. Präkelt, M. Wollenhaupt, A. Assion, Ch. Horn, C. Sarpe-Tudoran, M. Winter, and T. Baumert. *Rev. Sci. Instr.*. 74:4950, 2003.

32. J. D. McMullen. *J. Opt. Soc. Am.*, 67:1575, 1977.

33. M. Wollenhaupt, A. Assion, and T. Baumert. *Handbook of Lasers and Optics.* edited by F. Träger (Springer, New York), 2007.

34. L. Englert, B. Rethfeld. L. Haag, M. Wollenhaupt, C. Sarpe-Tudoran, and T. Baumert. Control of ionization processes in high band gap materials via tailored femtosecond pulses. *Optics Express*, 15:17855. 2007.

35. L. Englert, M. Wollenhaupt, L. Haag, C. Sarpe-Tudoran. B. Rethfeld, and T. Baumert. Material processing of dielectrics with temporally asymmetric shaped femtosecond laser pulses on the nanometer scale. *Appl. Phys. A*, accepted for publication, 2008.